Decreased ZO1 expression causes loss of time-dependent tight junction function in the liver of *ob/ob* mice

Yuya Tsurudome
Sanyo-Onoda City University: Sanyoonoda Shiritsu Yamaguchi Tokyo Rika Daigaku
Nao Morita
Sanyo-Onoda City University: Sanyoonoda Shiritsu Yamaguchi Tokyo Rika Daigaku
Michiko Horiguchi
Sanyo-Onoda City University: Sanyoonoda Shiritsu Yamaguchi Tokyo Rika Daigaku
Kentaro Ushijima (ushijima-kentarou@umin.ac.jp)
Sanyo-Onoda City University: Sanyoonoda Shiritsu Yamaguchi Tokyo Rika Daigaku
https://orcid.org/0000-0003-2637-3916

Research Article

Keywords: Diabetes, Liver, ZO1, Tight junction proteins, Diurnal variations

Posted Date: November 23rd, 2021

DOI: https://doi.org/10.21203/rs.3.rs-1085056/v1

Abstract

Diabetes patients are at a high risk of developing complications related to angiopathy and disruption of the signal transduction system. The liver is one of the multiple organs damaged during diabetes. Few studies have evaluated the morphological effects of adhesion factors in diabetic liver. The influence of diurnal variation has been observed in the expression and functioning of adhesion molecules to maintain tissue homeostasis associated with nutrient uptake. The present study demonstrated that the rhythm-influenced functioning of tight junction was impaired in the liver of *ob/ob* mice. The tight junctions of hepatocytes were loosened during the dark period in normal mice compared to those in *ob/ob* mice, where the hepatocyte gaps remained open throughout the day. The time-dependent expression of zonula occludens 1 (ZO1) in the liver plays a vital role in the functioning of the tight junction. The time-dependent expression of ZO1 was nullified and its expression was attenuated in the liver of *ob/ob* mice. ZO1 expression was inhibited at the mRNA and protein levels. The expression rhythm of ZO1 was found to be regulated by heat shock factor (HSF)1/2, the expression of which was reduced in the liver of *ob/ob* mice. The DNA-binding ability of HSF1/2 was decreased in the liver of *ob/ob* mice compared to that in normal mice. These findings suggest the involvement of impaired expression and functioning of adhesion factors in diabetic liver complications.

Introduction

Obesity associated with binge eating leads to the development of metabolic diseases, such as diabetes and dyslipidemia. Diabetes and obesity are strongly linked to the onset and progression of nonalcoholic fatty liver disease (NAFLD) and nonalcoholic steatohepatitis (NASH) [1]. Although NAFLD and NASH progress to fatty liver, there exists an underlying relationship between the alleviation of diabetes and NAFLD that could be exploited to establish liver-focused treatments [2]. Since diabetes patients are at a high risk of developing hepatitis and liver cancer [3], it is necessary to include a treatment protocol for NAFLD alongside with diabetes in these patients. Though therapies that focus on normalizing the abnormal metabolic system are in practice, satisfactory therapeutic outcomes have not been obtained. At present, research to analyze the morphological development of the liver is underway; however, several aspects remain to be elucidated.

Regardless of obesity, diabetes patients show high incidence of three major complications, namely, retinopathy, kidney disease, and peripheral neuropathic pain. Angiopathy is the major cause of these complications resulting from a disrupted capillary system [4], as seen from the analysis of tight junctions that act as barrier mechanisms. The expression of tight junction-forming factors was significantly reduced in the retina of diabetic mice [5]. Similarly, decreased expression of zonula occludens-1 (ZO1) in the small intestine of diabetic mice is associated with inflammation and endotoxin invasion [6]. The binding disorders of hepatic tight junction are also one of the risk factors for causing liver disease. Functionally, tight junctions in the liver prevent the leakage of bile from the bile duct and facilitate the uptake of nutrients [7]. However, the relationship between the alteration of liver-associated tight junctions and the associated pathological conditions remains unclear.

In the living system, factors linked to the defense and maintenance of homeostasis are controlled by the biological clock system. In type 2 diabetes, the expression amplitude of the clock gene, which is the core of the biological clock system, is attenuated [8]. Conversely, the onset of type 2 diabetes may cause an irregular rhythm in the membrane protein activity [9]. Therefore, elucidating the pathophysiology of diabetes warrants biochemical analysis based on the biological clock system. Since alteration in the expression of tight junction-related factors was dependent on the time difference [10], it was assumed that disrupted physiological time-dependency in diabetes would result in the abnormal expression of liver tight junction-related factors, leading to the pathological manifestation of hepatitis. This study aimed to evaluate and explore the mechanism associated with the transformation of altered liver tight junction function in diabetes using *ob/ob* mice.

Materials And Methods

Animal experiments

Six-week-old male C57BL/6J Ham Slc-*ob/ob* mice and age/sex-matched C57BL/6J Ham Slc-*+/+* mice (control mice) were purchased from the Japan SLC Inc. (Shizuoka, Japan). Mice were housed in a light-controlled room at a temperature of 24 ± 1 °C and 60 ± 10 % humidity, with food and water available ad libitum. In the light/dark cycle, zeitgeber time (ZT) with ZT0 and ZT12 were defined as time of lights on and off, respectively. During the dark period, a dim red light was used to aid in animal treatment.

Vascular permeability was assessed by intravenous (i.v) administration of Evans blue dye (30 mg/kg) at ZT0 and ZT12, according to previous reports [11]. After 1 h post-injection, the mice were euthanized and thoroughly perfused with 0.9 % saline to clear the circulation of any residual dye. The perfused liver was collected after fixation with 4 % paraformaldehyde. Frozen liver sections were processed for fluorescent microscopic evaluation and photographed with a BZ-9000 microscope. For the assessment of Evans blue infiltration, 100 mg of the liver was soaked in 500 µL of 4 % paraformaldehyde, incubated at 55 °C for a day (to extract Evans blue), and centrifuged; the absorbance of the supernatant was measured at 610 nm using an Infinite® 200 PRO plate reader (Tecan Group Ltd., Männedorf, CH).

Cell culture

Hepa1-6 cells were purchased from the Cell Resource Center for Biomedical Research (Tohoku University, Sendai, Japan). Cells were maintained in Dulbecco's modified Eagle's medium (DMEM; Gibco BRL, Paisley, UK) supplemented with 10 % fetal bovine serum (FBS; AFC Biosciences, Lenexa, KS, USA) and 50 U/mL penicillin/ 50 µg/ml streptomycin (Gibco) at 37 °C in a humidified 5 % CO_2 atmosphere.

RNA isolation and quantitative real-time polymerase chain reaction (qRT-PCR)

Total RNA was extracted from the mouse liver using the PureLink® RNA Mini Kit (Thermo Fisher Scientific, CA, USA) as per the manufacturer's instructions. Reverse transcription was performed with the PrimeScript™ RT reagent Kit (Takara Bio, Otsu, Japan). Real-time PCR was performed with TB Green®

Premix Ex Taq™ (Takara Bio) using the StepOnePlus™ Real-Time PCR System (Life Technologies, Carlsbad, CA, USA). All experiments that used kits were performed as per the manufacturer's instructions. The data were normalized to 18S ribosomal RNA gene (*Rn18s*) used as the internal control. Nucleotide sequences of specific primers of genes used in the study are listed in **Table 1**.

Table 1: Primer sets for qPCR analysis of gene expression

Gene name	*Accession ID*	*Primer*	*Sequence*
Tjp1	NM_001163574.1	F	CTCCGATCATTCCACGCAGT
		R	TTCGGTTCTGGAAGAGTGGG
Tjp2	NM_001198985.2	F	GGAGACCAGATTCTGAAGGTGAACACAC
		R	ACCTTTGGGGATTTCTAGCAGGTAGAGGAC
Occludin	NM_001360536.1	F	GATTCCGGCCGCCAAGGTT
		R	TGCCCAGGATAGCGCTGACT
Claudin 1	NM_016674.4	F	CACCGGGCAGATACAGTGCAA
		R	ATGCACTTCATGCCAATGGTGGA
Claudin 3	NM_009902.4	F	CCTCTATTCTGCGCCGCGAT
		R	CGACTGCTGGTAGTGGTGACG
Claudin 5	NM_013805.4	F	AGGATGGGTGGGCTTGATCCT
		R	GTACTCTGCACCACGCACGA
Rn18s	NR_003278.3	F	CGGCTACCACATCCAAGGAA
		R	GCTGGAATTACCGCGGCT

Protein extraction and western blotting

Hepatic membrane proteins were extracted from the mice liver using the FractionPREP™ cell fractionation kit (K270; Biovision, Mountain View, CA, USA) as per the manufacturer's instructions. Denatured samples containing 20 µg of each protein fraction were separated by sodium dodecyl sulfate-polyacrylamide gel electrophoresis (SDS-PAGE) and transferred onto a polyvinylidene difluoride membrane. Separated proteins were stained with Coomassie Brilliant Blue (CBB) as a control for equal loading of the membrane

fraction. The membranes were incubated with primary antibodies: anti-ZO1 (1:1000; ab15602; Abcam, Cambridge, UK). Specific antigen-antibody complexes were visualized using HRP-conjugated anti-rabbit IgG (1:10000; sc-2032; Santa Cruz Biotechnology, Santa Cruz, CA) and ImmunoStar LD (Wako Chemicals, Osaka, Japan). Visualized images were scanned by a BIO-RAD ChemiDoc™ Touch Imaging System (Bio-Rad, Hercules, CA, USA).

Transcriptional activity assay

Mouse heat shock factor 1 (HSF1) and HSF2 expression vectors were purchased from OriGene (HSF1: MR208087, HSF2: MR208286, Guangzhou, China). Mouse tight junction protein 1 (m*Tjp1*)-reporter vectors containing the *mTjp1* promoter region spanning from -650 to +50, -248 to +50, and -50 to +50 (relative to the transcription start site, +1) were constructed using the VectorBuilder services (VectorBuilder Inc, Chicago, IL, USA). Hepa1-6 cells were seeded at a density of 2×10^4 cells/well in 24-well culture plates. Cells were transfected with 50 ng of the green fluorescent protein (GFP) reporter construct and 500 ng (total) of the respective expression vector using Lipofectamine® 3000 Reagent (Thermo Fisher Scientific). The pCMV-6 empty vector was added to obtain a constant final DNA concentration in all transfections. After 24 h post-transfection, the fluorescence intensity was analyzed using an Infinite® 200 PRO plate reader (Tecan Group Ltd.). The ratio of GFP intensity to protein concentration in each sample served as a measure of normalization.

Chromatin immunoprecipitation (ChIP) analysis

ChIP assay was performed with reference to past papers [12]. Cross-linked chromatin from liver was sonicated on ice and nuclear fractions were obtained by centrifugation at 10,000 × g for 5 min. Supernatants were incubated with the following antibodies: anti-HSF1 (1:200; ab16502; Abcam), anti-HSF2 (1:200; ab32360; Abcam), or rabbit anti-IgG (1:200; sc66931; Santa Cruz Biotechnology). DNA was purified using the DNA purification kit (Promega, Madison, WI, USA) as per the manufacturer's instructions and amplified by PCR for the surrounding HSF response element (HSE) in the 5' -flanking region of the mouse *Tjp1* gene. Primer sequences used for amplification were as follows: forward, 5'-AATGGTATGGCATAGGAGTGG -3'; and reverse, 5'- TTACGCTTGACAAAGAGGAAG-3'. TB green premix Ex Taq™ (Takara Bio) with the StepOnePlus™ Real-Time PCR System (Life Technologies) was used to quantify the products. All data were normalized to the PCR products of input DNA. The quantitative reliability of PCR was evaluated by kinetic analysis of the amplified products to ensure that signals were derived exclusively from the exponential phase of amplification. ChIP was performed either in the absence of antibodies or in the presence rabbit IgG as a negative control.

Statistical analyses

All data are expressed as mean ± standard error of the mean (SEM). Statistical analyses were performed using the GraphPad Prism software (ver. 8; GraphPad Software, San Diego, CA, USA). Differences among the groups were analyzed by two-way ANOVA, followed by Tukey's post-hoc and Sidak's post-hoc tests. $P < 0.05$ was considered statistically significant. Although no statistical methods were used to predetermine

the sample size, the sample sizes used in the present study are similar to those reported in previous studies [6, 9, 13]. The experiments were not randomized.

Results

Attenuation of time dependency of tight junctions in the mouse diabetic liver

To examine possible alterations in the diurnal variation of tight junctions in the diabetic liver, vascular leakage was analyzed using Evans blue in wild-type and *ob/ob* mice. Fluorescent microscopic analysis revealed dark period-dependent permeation of Evans blue in the hepatic parenchymal cells of wild-type and time independent increase of Evans blue permeation in the liver of *ob/ob* mice (Fig. 1a, b). These results indicate attenuated time dependency and tight junction functions in the diabetic liver, in vivo.

Influence of diabetes on the expression of tight junction-related genes in the mouse liver

Tight junctions are adhesion sites on the cell membrane that are densely packed with multiple interacting proteins. Although the attenuation of the expression of tight junction factor, ZO1, has been deciphered in *ob/ob* mice, the time-dependent changes remain to be elucidated. To identify the attenuated genes associated with diurnal variation in diabetes, the mRNA expression levels of significant tight junction-related genes were evaluated. Accordingly, the expression levels of *Tjp1*, *Tjp2*, *occludin* (*Ocln*), *claudin 1* (*Cldn1*), *Cldn3*, and *Cldn5* were measured. The expression of *Tjp1* mRNA was significantly decreased in the light periods in *ob/ob* mice (Fig. 2a-f). Since the time dependency of ZO1 expression was attenuated in *ob/ob* mice, we speculated that ZO1 might play a central role in the time dependency of tight junctions in diabetes.

The expression of *Tjp1* mRNA exhibited significant diurnal time-dependency in the liver of wild-type mice maintained under light/dark cycle conditions (Fig. 2a). The plasmalemmal expression of ZO1 indicated significant time dependence similar to that of the mRNA expression in the liver of wild-type mice (Fig. 3a, b). The expression of *Tjp1* mRNA and ZO1 protein was continually decreased throughout the day in the liver of *ob/ob* mice compared to that of the wild-type mice (Fig. 2a, 3b). These results indicate that decreased of ZO1 expression causes a decrease in hepatic tight junction function in *ob/ob* mice.

Transcriptional regulation of Tjp1 by HSFs

Sequence analysis of the promoter region of *Tjp1* genes revealed a highly conserved HSE located between -468 and -448 base pairs (bp) upstream from the transcription start site (relative to the transcription start site, +1) (Fig. 4a). Further, the repression of *Tjp1* transcription by HSFs was explored. The activity of *Tjp1* reporters was diminished by the elimination of their promoter sequences (Fig. 4b). Although the reporter assay revealed that cells cotransfected with *Tjp1:(-650/+50)* reporter vector or *Tjp1:(-248/+50)* reporter vector and HSF1/2 had high fluoresence, cells cotransfected with *Tjp1:(-50/+50)* reporter vector and HSF1/2 had slightly increased fluoresence compared with cells cotransfected with

Tjp1:(-50/+50) reporter vector and pCMV-6. These results suggest that the HSFs element within −468 to -448 bp was important for *Tjp1* transcriptional regulation (Fig. 4b). The *Tjp1:(-248/+50)* reporter also showed 5 times the transcriptional activity of the control due to the presence of single HSFs response element. Since the HSFs transcription mechanism requires multiple HSFs response elements [14], it was considered that the HSF region near −468 to -448 bp is involved in the *Tjp1* transcription.

To confirm whether the transcriptional ability of HSFs affects the time-dependent expression of ZO1, the nuclear expression level of HSF1/2 was measured in the liver of *ob/ob* mice. The expression of *Hsf1/2* mRNA indicated significant time dependence in the liver of wild-type mice (Fig. 4c). In contrast, the expression of H *Hsf1/2* mRNA was continually decreased throughout the day in the liver of *ob/ob* mice (Fig. 4c). ChIP analysis demonstrated significantly enhanced binding of HSF1/2 to the promoter region of the gene containing the HSEs at dark phase compared to that observed at light phase in the liver of wild-type mice (Fig. 4d). In contrast, the amount of HSF1/2 binding to the *Tjp1* promoter in the liver of *ob/ob* mice was decreased in both light and dark phases (Fig. 4d). These results indicate that the decrease in HSF1/2 expression during diabetes mellitus eliminates the time-dependent expression fluctuation of ZO1 and disrupts the tight junction mechanism of the liver.

Discussion

Morphological wear or physiological effects, including angiopathy and modulation of insulin signals, are associated with the complications linked with tissue damage in diabetes [4, 15]. In this study, we found that the formation of tight junctions was diminished because of the decreased of ZO1 expression in the liver of diabetic mice. The results indicate a loss of function of the defense mechanism in healthy hepatocytes due to attenuated diurnal variability in diabetic liver.

Vascular permeability associated with angiopathy is evaluated using Evans blue because of its high binding affinity to albumin and retention in the blood. The perisinusoidal space or space of Disse in the liver is a region around the sinusoid where plasma collects, and hence with the highest retention of Evans blue compared to all other tissues [16]. The space of Disse is liver-specific and serves as a site that expresses several transporters and facilitates the uptake of nutrients, such as fatty and amino acids [17]. The expansion of the space of Disse causes damage to the hepatic morphology and leads to the development of liver damage [18]. Since vascular permeability was enhanced, both in the resting and active period in diabetic mice, it was considered as an indication for the occurrence of possible liver damage.

Tight junctions in the liver are essential for maintaining the physiological function and hence, abnormal functioning of the same is associated with liver diseases [19]. Few studies have defined tight junction-related factors that are altered in liver diseases. The expression of ZO1, a protein that forms tight junctions, is downregulated in liver diseases, such as NASH and hepatic cancer [20, 21]. The expression of ZO1 was decreased in *ob/ob* mice, suggesting the possibility of NASH-related liver damage in diabetes, as proven clinically.

Reduction of HSF1 and HSF2 expression leads to liver injury. In HSF1 knockout mice, increased cytokine production and decreased clearance of reactive oxygen species, exacerbates the progression of hepatitis [25]. HSF2 positively regulates Psmb5 expression constituting 20S core proteasome complex; which suggests that Decreased proteasome activity is associated with liver fat accumulation and liver disease [26, 27]. Attenuated expression of HSFs increased the signals involved in promoting hepatitis in *ob/ob* mice. HSF1 drives the cascade of heat shock proteins which affects the expression of genes with downstream physiological functions. HSF1 binds to clock genes and controls the circadian clock mechanism in living organisms [22]. HSF1 functions as resetting the biological clock mechanism affected by changes in temperature and UV stimulation [23]. The amplitude of the clock gene expression reduces in *ob/ob* mice [24], but its association with HSF1 remains unclear. The expression of the clock gene may be related to the decrease in HSF1 expression (Fig. 4c-d), which causes liver injury in *ob/ob* mice.

Complications associated with systemic organs have been reported in people with diabetes. Several studies have focused on the signaling mechanism associated with the suggested risk of development of hepatitis. However, morphological evaluation and differential expression profiles of the liver during the course of diabetes have not been elucidated. The present study characterizes the morphological changes induced by diabetes in the liver and elucidates a novel mechanism involving cell-binding disorders in diabetes.

Declarations

Fundings

This work was supported by KAKENHI Grant-in-Aid for Young Scientists (20K19715) to Y.T., KAKENHI Grant-in-Aid for Research Activity Start-up (19K23832) to Y.T., and KAKENHI Grant-in-Aid for Fundamental Research(C) (19K07327) to K.U.

Author contributions

All authors (Y.T., N.M., M.H., and K.U.) participated in designing the study, interpreted the data and contributed to the writing and/or revising the manuscript. Y.T., N.M., and K.U. performed research, and Y.T. and K.U. analyzed data.

Data availability

The datasets analyzed during the current study are available from the corresponding author on reasonable request.

Conflict of interest

The authors state that there are no conflicts of interest to disclose.

Ethics approval

Animals in this study were treated according to the guidelines stipulated by the Animal Care and Use Committee of the Sanyo-Onoda City University. All experiments were conducted under the protocol approved by the Internal Committee for Animal Experiments at Sanyo-Onoda City University (approved protocol ID #A-2020-13-A).

References

Figures

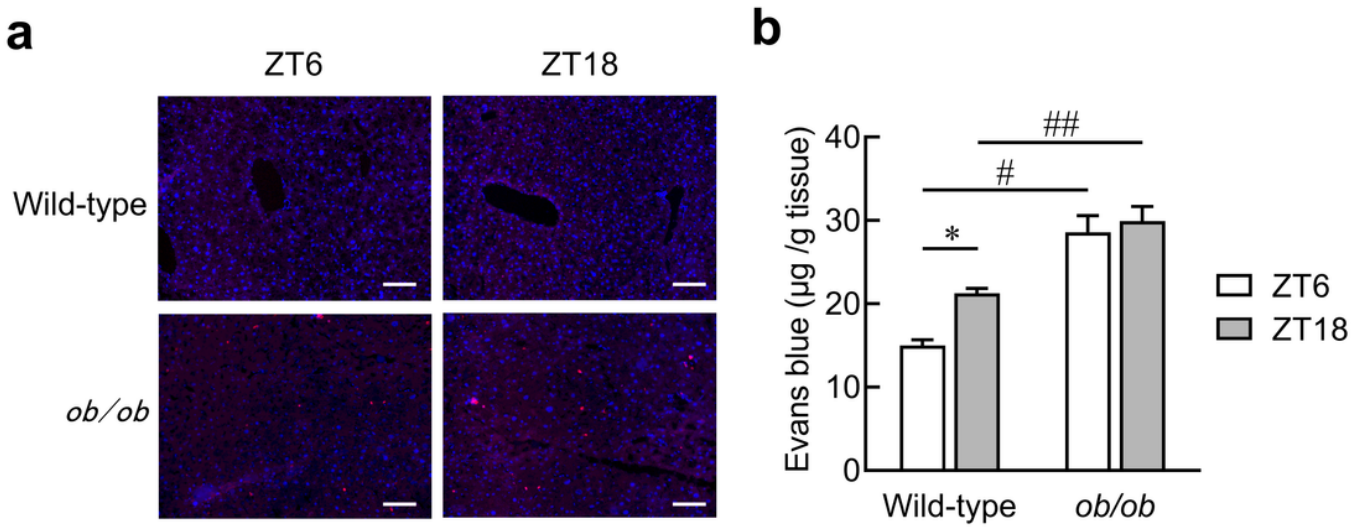

Figure 1

Tight junction dysfunction in the liver of ob/ob mice. (a) Representative image showing Evans blue fluorescence that evaluates the tight junction ability of liver tissue. Nuclei were also stained with 4'6-diamidino-2-phenylindole (blue). Scale bars indicate 50 μm. Data were collected for more than three mice in each group. (b) Quantification of Evans blue infiltrated into liver tissue. The data are expressed as μg of Evans blue per liver weight (g) and represent the mean ± SEM of 5 mice. *, $P < 0.05$; significantly different between the two groups; #, $P < 0.05$, ##, $P < 0.01$; significantly different from wild-type mice at the corresponding time points (two-way ANOVA with Tukey post hoc test).

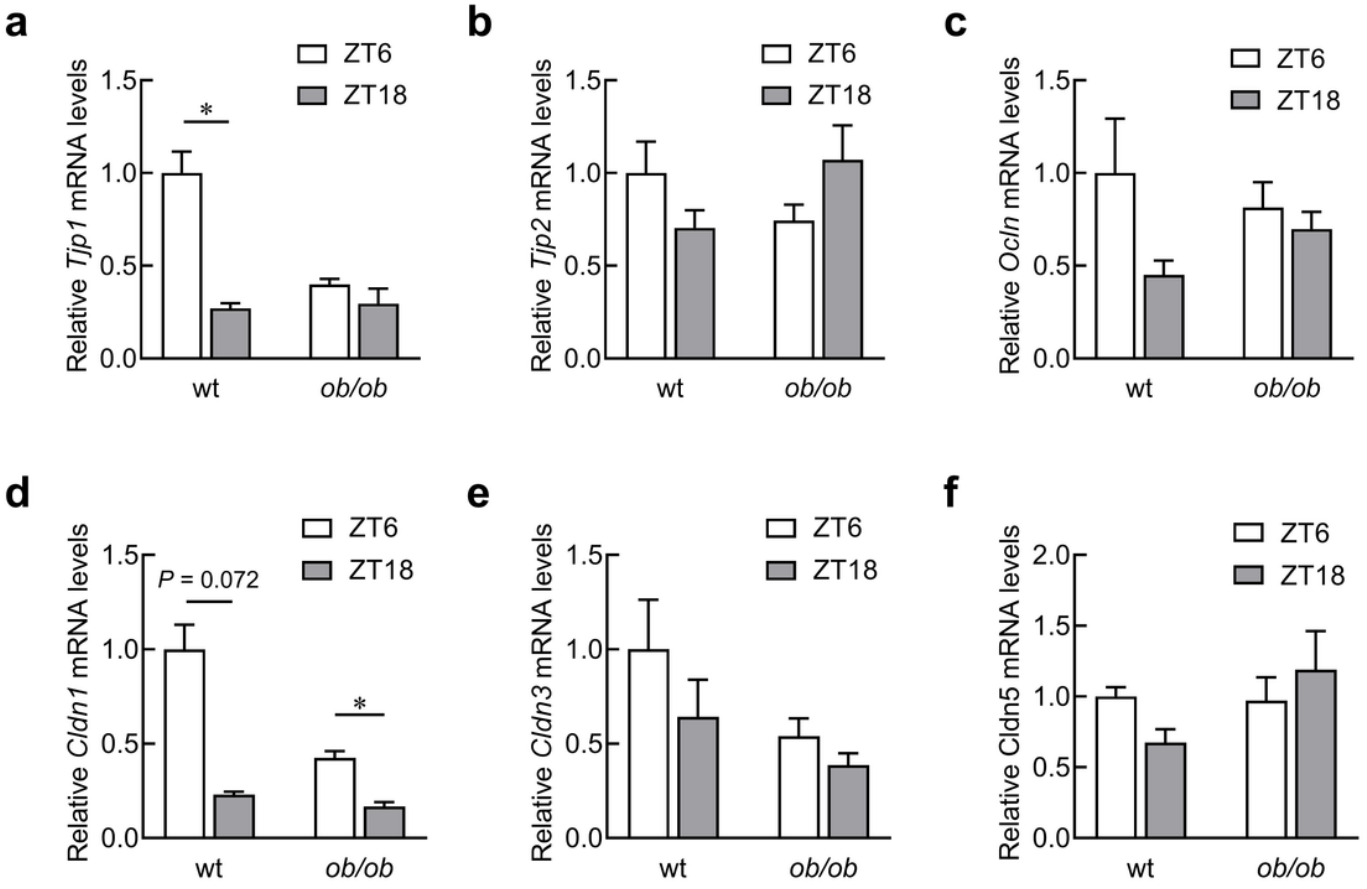

Figure 2

Time-dependent expression of hepatic tight junction related gene in ob/ob mice. Temporal expression profiles of Tjp1 (a), Tjp2 (b), Ocln (c), Cldn1 (d), Cldn3 (e), and Cldn5 (f) mRNA in the liver of wild-type and ob/ob mice. Values are shown as means with S.E.M. (n = 3). *P < 0.05; significantly different between the two groups (two-way ANOVA with Tukey post hoc test).

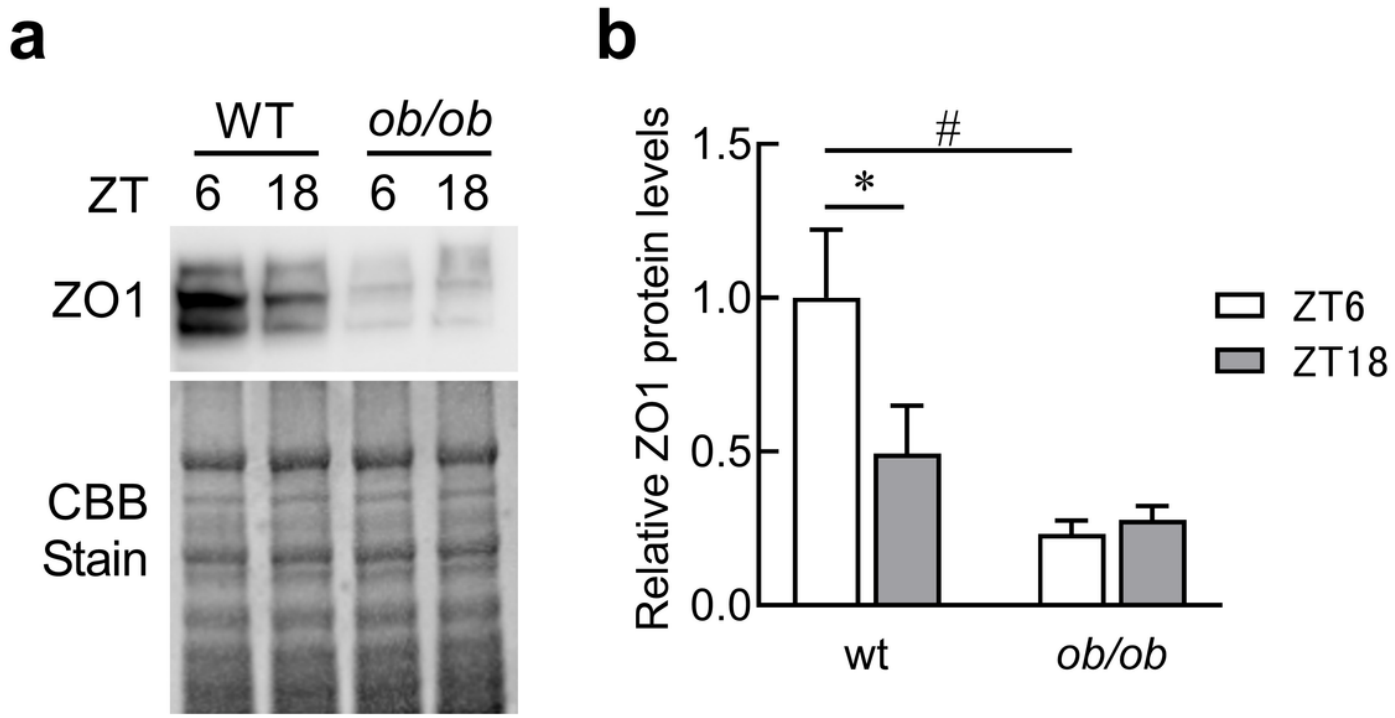

Figure 3

Influence of diabetes on the expression of ZO1 protein in the liver of mouse. (a, b) Temporal expression profiles ZO1 protein in the liver of wild-type and ob/ob mice. Values are shown as means with S.E.M. (n = 3). *, $P < 0.05$; significantly different between the two groups; #, $P < 0.05$ significantly different from wild-type mice at the corresponding time point (two-way ANOVA with Tukey post hoc test). CBB stain indicates the equal loading of proteins from the membrane fraction.

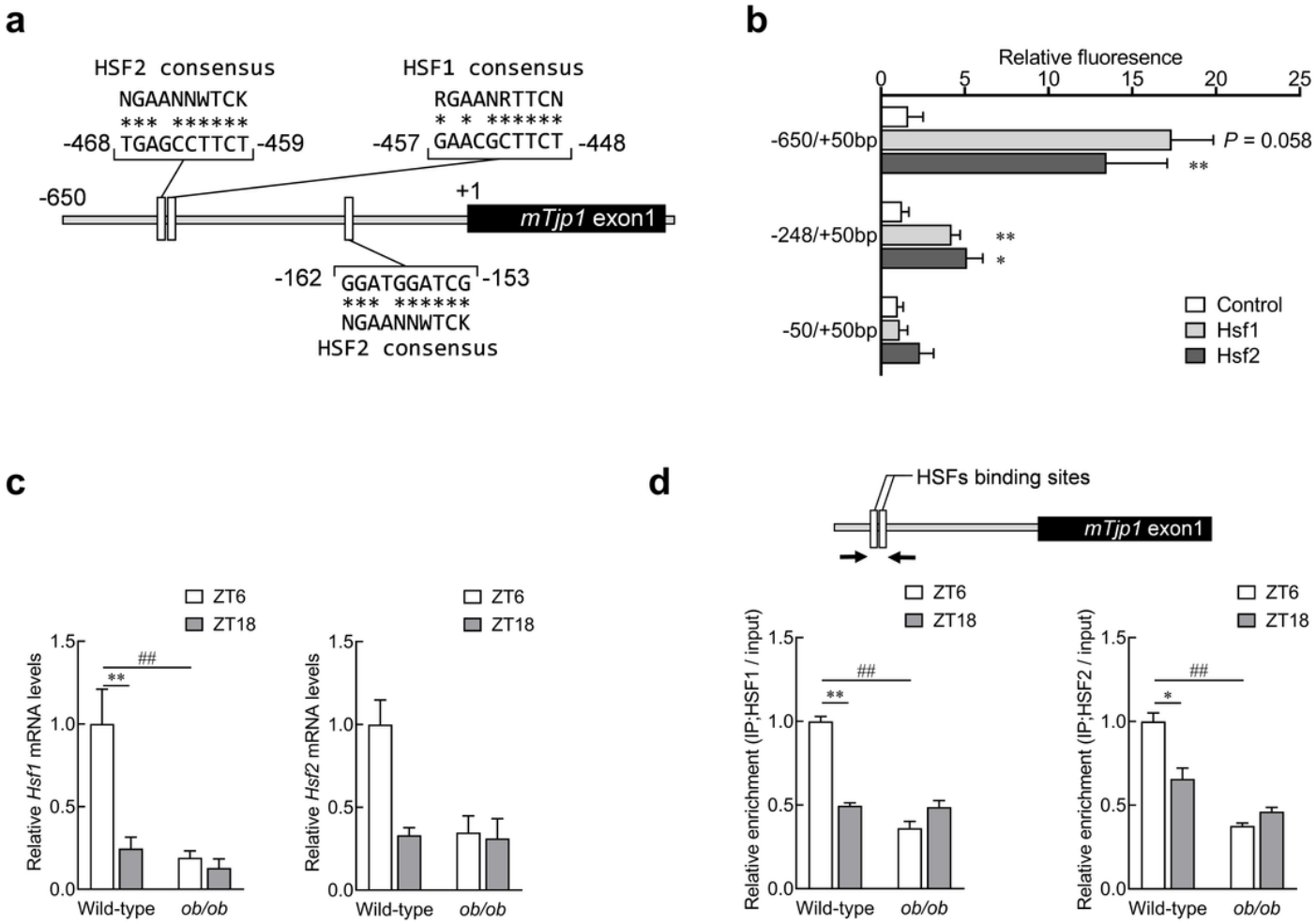

Figure 4

Time-dependent transcriptional regulation of Tjp1 gene by HSFs. (a) Location of consensus sequences for HSF response element within the mouse Tjp1 promoter region. The number of nucleotide residues indicates the distance from the transcription start site. (b) Temporal profiles of HSFs binding to the promoter region of the mouse Tjp1 gene in the liver of wild-type and ob/ob mice. *P < 0.05, **P < 0.01; significantly different from the control (two-way ANOVA with Tukey post hoc test). (c) Temporal expression profiles of Hsf1 and Hsf2 mRNA in the liver of wild-type and ob/ob mice. Values are shown as means with S.E.M. (n = 3). *, P < 0.05, ** P < 0.01; significantly different between the two groups; ##, P < 0.01; significantly different from wild-type mice at the corresponding time point (two-way ANOVA with Tukey post hoc test). (d) Temporal-binding profiles of HSF1 and HSF2 to the Tjp1 promoter in the liver of wild-type and ob/ob mice. Values are shown as means with S.E.M. (n = 4). *, P < 0.05; ** P < 0.01; significantly different between the two groups; ##, P < 0.01; significantly different from wild-type mice at the corresponding time point (two-way ANOVA with Tukey post hoc test).